JOURNAL OF THE AMERICAN CHEMICAL SOCIETY

Article

Nano-Segregated Polymeric Film Exhibiting High Ionic Conductivities

Kenji Kishimoto, Tomoyuki Suzawa, Tomoki Yokota, Tomohiro Mukai, Hiroyuki Ohno, and Takashi Kato

J. Am. Chem. Soc., **2005**, 127 (44), 15618-15623• DOI: 10.1021/ja0549594 • Publication Date (Web): 14 October 2005

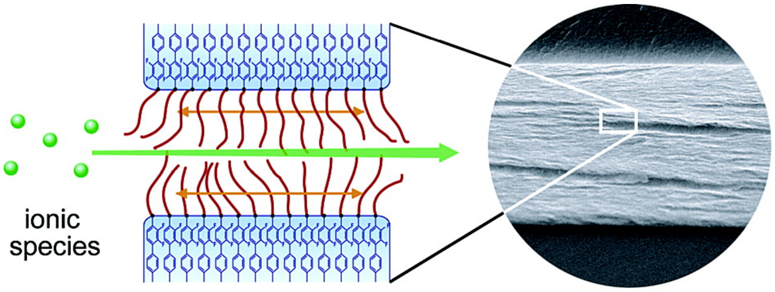

fast ion-conductive materials

Journal of the American Chemical Society is published by the American Chemical Society. 1155 Sixteenth Street N.W., Washington, DC 20036

JACS
ARTICLES

Nano-Segregated Polymeric Film Exhibiting High Ionic Conductivities

Kenji Kishimoto,[†] Tomoyuki Suzawa,[†] Tomoki Yokota,[†] Tomohiro Mukai,[‡]
Hiroyuki Ohno,[‡] and Takashi Kato*,[†]

*Department of Chemistry and Biotechnology, School of Engineering, The University of Tokyo,
Hongo, Bunkyo-ku, Tokyo 113-8656, Japan, and Department of Biotechnology, Tokyo University
of Agriculture and Technology, Nakacho, Koganei, Tokyo 184-8588, Japan*

Received July 23, 2005; E-mail: kato@chiral.t.u-tokyo.ac.jp

Abstract: Nanostructures can be used for the fabrication of highly functional materials transporting ions and charges. We demonstrate a new design strategy for polymeric higher ion-conductors. Phase-segregated layers of alternating mobile tetra(ethylene oxide)s (TEOs) and rigid aromatic cores where the TEO moieties are grafted from aromatic layers have been shown to be efficient to transport lithium triflate. Such segregated structures at the nanometer scale (nano-segregated structures) were prepared by in-situ photopolymerization of an aligned methacrylate liquid crystalline monomer comprising a terphenyl rigid rod mesogen having a TEO terminal chain. The ion-conductive TEO moiety remains in the highly mobile state even after polymerization, which is indicated by its low glass transition temperature (−45 °C). This nanostructured film exhibits an ionic conductivity parallel to the layer of 10^{-3} S cm^{-1} at room temperature. The highest ionic conductivity is in the level of 10^{-2} S cm^{-1} observed at 150 °C. The anisotropic ionic conductivities have been observed for the nano-segregated film.

Introduction

Self-organized nanostructures of liquid crystals can be applied to anisotropically functional materials.[1−29] Supramolecular assembly of molecules and nano-segregation can be used for the preparation of such anisotropic materials.[1−10] These materials have great potential as low-dimensional conductors of electrons[2,11−15] and ions[2,16−29] due to their phase-segregated structures. Macroscopic alignment of phase-segregated ordered nanostructures consisting of conductive and insulating parts is essential for efficient transportation. However it was not easy

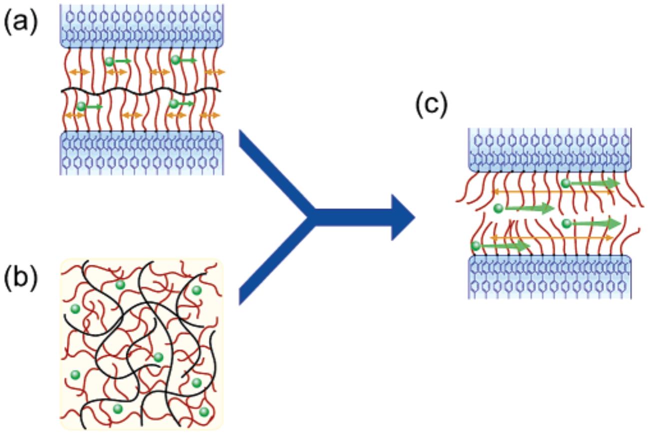

Figure 1. Design strategy for higher ion-conductive polymeric films. (a) Liquid crystalline ion-conductive nanostructured polymers having oligo(ethylene oxide) chains (indicated in red) as spacer units of the side chains. (b) Comb-shaped polymers having flexible ion-conductive oligo(ethylene oxide) side chains (in red). (c) Combined design of the advantages of (a) and (b): a new type of liquid crystalline nanostructured ion-conductor. The nanolayers consist of liquidlike ion-conductive (in red) and rigid aromatic mesogenic (in blue) domains.

[†] The University of Tokyo.

[‡] Tokyo University of Agriculture and Technology.

(1) (a) Special section of liquid crystals: *Curr. Opin. Solid State Mater. Sci.* **2002**, *6*, 513−587. (b) Hoeben, F. J. M.; Jonkheijm, P.; Meijer, E. W.; Schenning, A. P. H. J. *Chem. Rev.* **2005**, *105*, 1491−1546. (c) van Nostrum, C. F.; Nolte, R. J. M. *Chem. Commun.* **1996**, 2385−2392. (d) Stupp, S. I.; LeBonheur, V.; Walker, K.; Li, L. S.; Huggins, K. E.; Keser, M.; Amstutz, A. *Science* **1997**, *276*, 384−389. (e) *Side Chain Liquid Crystal Polymer*; McArdle, C. B., Ed.; Blackie: London, 1989. (f) Lehn, J. M. *Makromol. Chem. Macromol. Symp.* **1993**, *36*, 1−17. (g) Kato, T.; Fréchet, J. M. J. *Macromol. Symp.* **1995**, *98*, 311−326.

(2) Kato, T. *Science* **2002**, *295*, 2414−2418.

(3) Ikkala, O.; ten Brinke, G. *Chem. Commun.* **2004**, 2131−2137.

(4) Pollino, J. M.; Weck, M. *Chem. Soc. Rev.* **2005**, *34*, 193−207.

(5) Saez, I. M.; Goodby, J. W. *J. Mater. Chem.* **2005**, *15*, 26−40.

(6) Tschierske, C. *J. Mater. Chem.* **2001**, *11*, 2647−2671.

(7) Lee, M.; Cho, B.-K.; Zin, W.-C. *Chem. Rev.* **2001**, *101*, 3869−3892.

(8) Barberá, J.; Puig, L.; Romero, P.; Serrano, J. L.; Sierra, T. *J. Am. Chem. Soc.* **2005**, *127*, 458−464.

(9) McCubbin, J. A.; Tong, X.; Wang, R.; Zhao, Y.; Snieckus, V.; Lemieux, R. P. *J. Am. Chem. Soc.* **2004**, *126*, 1161−1167.

(10) Kato, T.; Matsuoka, T.; Nishii, M.; Kamikawa, Y.; Kanie, K.; Nishimura, T.; Yashima, E.; Ujiie, S. *Angew. Chem., Int. Ed.* **2004**, *43*, 1969−1972.

(11) Simpson, C. D.; Wu, J.; Watson, M. D.; Müllen, K. *J. Mater. Chem.* **2004**, *14*, 494−504.

(12) Bushey, M. L.; Hwang, A.; Stephens, P. W.; Nuckolls, C. *Angew. Chem., Int. Ed.* **2002**, *41*, 2828−2831.

(13) Boden, N.; Bushby, R. J.; Clements, J. *J. Chem. Phys.* **1993**, *98*, 5920−5931.

(14) Messmore, B. W.; Hulvat, J. F.; Sone, E. D.; Stupp, S. I. *J. Am. Chem. Soc.* **2004**, *126*, 14452−14458.

(15) Smith, R. C.; Fischer, W. M.; Gin, D. L. *J. Am. Chem. Soc.* **1997**, *119*, 4092−4093.

(16) Percec, V.; Heck, J. A.; Tomazos, D.; Ungar, G. *J. Chem. Soc., Perkin Trans. 2* **1993**, 2381−2388.

(17) Percec, V.; Tomazos, D. *J. Mater. Chem.* **1993**, *3*, 633−642.

(18) Yoshio, M.; Mukai, T.; Kanie, K.; Yoshizawa, M.; Ohno, H.; Kato, T. *Adv. Mater.* **2002**, *14*, 351−354.

(19) Yoshio, M.; Mukai, T.; Ohno, H.; Kato, T. *J. Am. Chem. Soc.* **2004**, *126*, 994−995.

10.1021/ja0549594 CCC: $30.25 © 2005 American Chemical Society

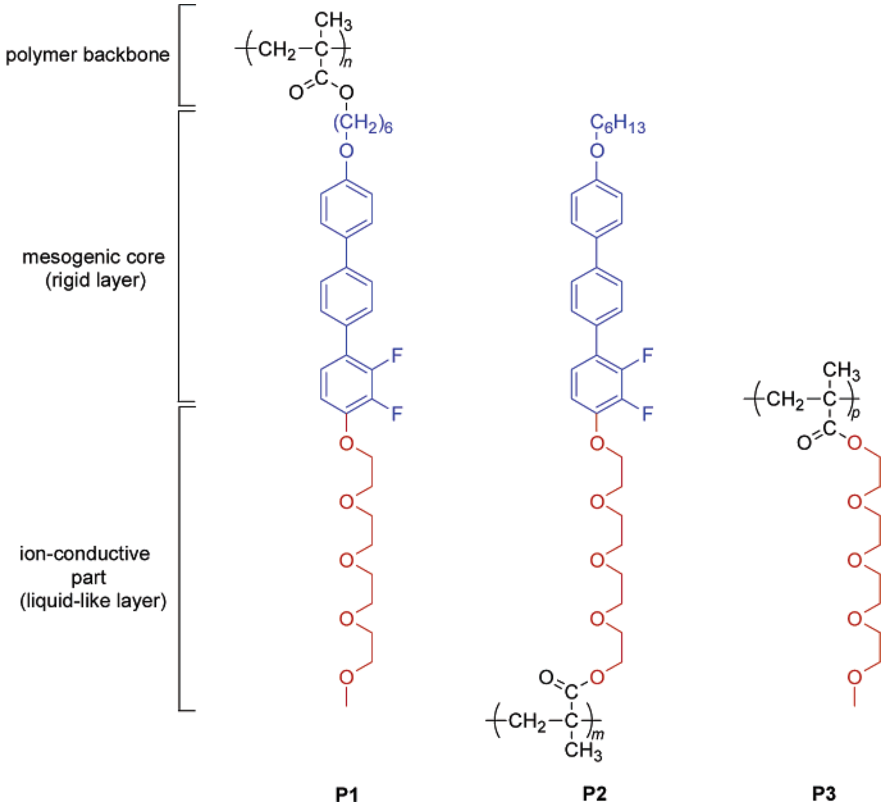

Figure 2. Molecular structures of ion-conductive polymers.

to control macroscopically oriented structures of liquid crystals to achieve desired functions. Recently, we have reported that the self-assembly of block molecules consisting of ion-conductive oligo(ethylene oxide)s and ion-insulating mesogenic rod parts leads to the formation of two-dimensional (2-D) ion-conductors.[25−29] They exhibit anisotropic ion conduction due to the homeotropic alignment in the liquid crystalline (LC) smectic phases on the substrates. Such nanostructures were fixed by in-situ photopolymerization of a block liquid crystalline monomer having a tetra(ethylene oxide) (TEO) moiety, which results in the fabrication of self-standing 2-D nanostructured films (Figure 1a).[25] However, the ionic conductivities still remained at values of less than 10^{-5} S cm^{-1} at room temperature. We predicted that the ionic conductivity should increase for polymeric self-standing films if a faster molecular motion of the ion-conductive parts is achieved. For non-LC poly(ethylene oxide)-based (PEO-based) ion-conductors, several approaches to improving the motion of ion-conductive moieties have been reported.[30−37] For example, polymers with side chains of oligo(ethylene oxide)s were developed to improve ionic conductivities (Figure 1b). In these polymers, the depression of the glass transition temperatures (T_g) of the oligo(ethylene oxide)s or the suppression of the crystallization of the molecules was intended for solid-state materials.[34−37] Although this design led to the enhancement of the motion of ethylene oxide chains, their ionic conductivities were also limited below 10^{-5} S cm^{-1} at room temperature.[37]

We here demonstrate the new design of an anisotropic polymeric ion-conductive film exhibiting high ionic conductivities of a value of 10^{-3} S cm^{-1} at room temperature. This film has formed a layered nano-segregated structure consisting of alternating a highly mobile ion-conductive part and a rigid mesogenic part.

Results and Discussion

The design strategy for anisotropic higher ion-conductive polymeric films in the present study is shown in Figure 1. The key for such organization presented in Figure 1c is to use the molecular structure of **P1** shown in Figure 2. **P1** consists of three molecular blocks: a polymer backbone, a mesogenic aromatic core, and a TEO part (Figure 2). In particular, the TEO

---

(20) Hoshino, K.; Yoshio, M.; Mukai, T.; Kishimoto, K.; Ohno, H.; Kato, T. *J. Polym. Sci., Part A: Polym. Chem.* **2003**, *41*, 3486−3492.
(21) Mukai, T.; Yoshio, M.; Kato, T.; Yoshizawa, M.; Ohno, H. *Chem. Commun.* **2005**, 1333−1335.
(22) Cho, B.-K.; Jain, A.; Gruner, S. M.; Wiesner, U. *Science* **2004**, *305*, 1598−1601.
(23) Cho, B.-K.; Jain, A.; Nieberle, J.; Mahajan, S.; Wiesner, U.; Gruner, S. M.; Türk, S.; Räder, H. J. *Macromolecules* **2004**, *37*, 4222−4234.
(24) Beginn, U.; Zipp, G.; Mourran, A.; Walther, P.; Möller, M. *Adv. Mater.* **2000**, *12*, 513−516.
(25) Kishimoto, K.; Yoshio, M.; Mukai, T.; Yoshizawa, M.; Ohno, H.; Kato, T. *J. Am. Chem. Soc.* **2003**, *125*, 3196−3197.
(26) Ohtake, T.; Ogasawara, M.; Ito-Akita, K.; Nishina, N.; Ujiie, S.; Ohno, H.; Kato, T. *Chem. Mater.* **2000**, *12*, 782−789.
(27) Ohtake, T.; Takamitsu, Y.; Ito-Akita, K.; Kanie, K.; Yoshizawa, M.; Mukai, T.; Ohno, H.; Kato, T. *Macromolecules* **2000**, *33*, 8109−8111.
(28) Ohtake, T.; Ito, K.; Nishina, N.; Kihara, H.; Ohno, H.; Kato, T. *Polym. J.* **1999**, *31*, 1155−1158.
(29) Hoshino, K.; Kanie, K.; Ohtake, T.; Mukai, T.; Yoshizawa, M.; Ujiie, S.; Ohno, H.; Kato, T. *Macromol. Chem. Phys.* **2002**, *203*, 1547−1555.
(30) Tarascon, J.-M.; Armand, M. *Nature* **2001**, *414*, 359−367.
(31) Meyer, W. H. *Adv. Mater.* **1998**, *10*, 439−448.
(32) Takeoka, S.; Ohno, H.; Tsuchida, E. *Polym. Adv. Technol.* **1993**, *4*, 53−73.
(33) Hawker, C. J.; Chu, F.; Pomery, P. J.; Hill, D. J. T. *Macromolecules* **1996**, *29*, 3831−3838.
(34) Matsumi, N.; Mizumo, T.; Ohno, H. *Chem. Lett.* **2004**, 372−373.
(35) Nishimoto, A.; Agehara, K.; Furuya, N.; Watanabe, T.; Watanabe, M. *Macromolecules* **1999**, *32*, 1541−1548.
(36) Cowie, J. M. G.; Martin, A. C. S. *Polym. Commun.* **1985**, *26*, 298−300.
(37) Buriez, O.; Han, Y. B.; Hou, J.; Kerr, J. B.; Qiao, J.; Sloop, S. E.; Tian, M.; Wang, S. *J. Power Source* **2000**, *89*, 149−155.

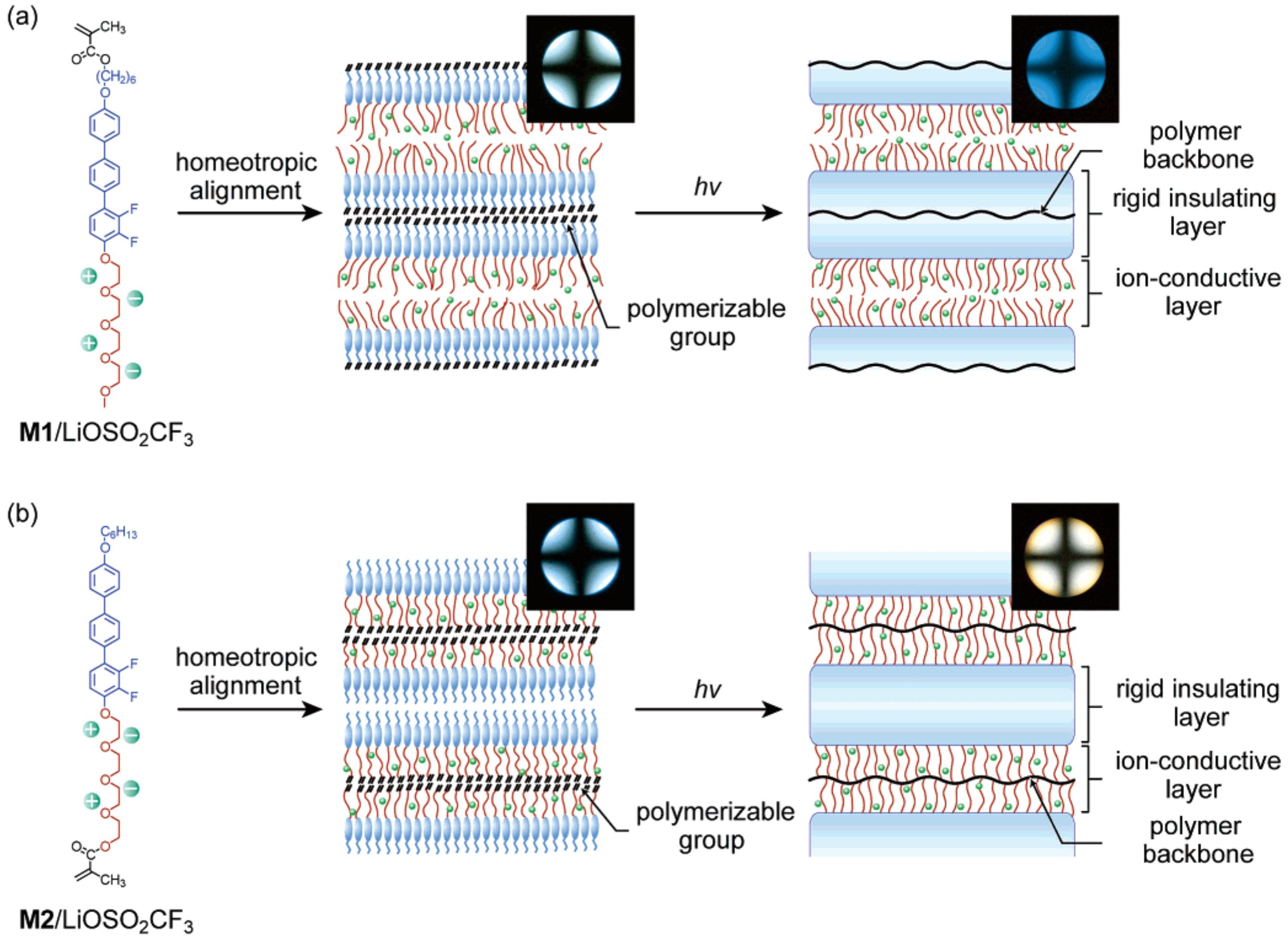

Figure 3. Preparation of macroscopically oriented and nano-segregated ion-conductive polymeric films. (a) Molecular structure of **M1**/$LiOSO_2CF_3$ (left), homeotropically oriented **M1**/$LiOSO_2CF_3$ in the smectic A phase (60 °C) on the substrate (center), and oriented nano-segregated structure of **P1**/$LiOSO_2CF_3$ with a highly mobile TEO moiety (right); (b) molecular structure of **M2**/$LiOSO_2CF_3$ (left), oriented **M2**/$LiOSO_2CF_3$ in the smectic A phase (80 °C) (center), and nano-segregated structure of **P2**/$LiOSO_2CF_3$ where the motion of the TEO moiety is restricted by the rigid insulating layer and polymer backbones (right).

Scheme 1. Synthesis of Mesogenic Cores

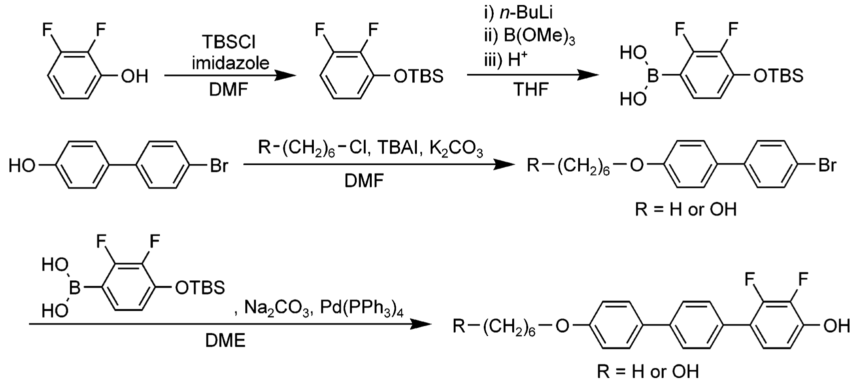

chain is introduced on to the extremity of the rigid aromatic core to achieve high segmental motion of the chains. The nanolayered structure shown in Figure 1a for **P2** and the side-chain polymer of low T_g shown in Figure 1b have been combined for the design of **P1** to achieve the formation of ion-conductive paths consisting of highly mobile liquidlike organized layers (Figure 1c).

The target nanostructure of the film shown in Figure 1c was fixed by the in-situ photopolymerization of a homeotropic monodomain formed by an LC monomer (**M1**) (Figure 3a).

Synthesis. Synthetic routes of liquid crystalline monomers are shown in Schemes 1−3. Compounds **M1** and **M2** were prepared by etherification of terphenyl mesogenic compounds[38] (Scheme 1) and tetra(ethylene oxide) derivatives, followed by esterification with methacryloyl chloride under light-resistant condition (Schemes 2 and 3). The terphenyl mesogenic cores

---

[38] (a) Gray, G. W.; Hird, M.; Lacey, D.; Toyne, K. J. *J. Chem. Soc., Perkin Trans. 2* **1989**, 2041−2053. (b) Dong, C. C.; Hird, M.; Goodby, J. W.; Styring, P.; Toyne, K. J. *Ferroelectrics* **1996**, *180*, 245−257. (c) Mehl, G. H.; Kouwer, P. H. J. *Angew. Chem., Int. Ed.* **2003**, *42*, 6015−6018.

Scheme 2. Synthesis of Liquid Crystalline Monomer **M1**

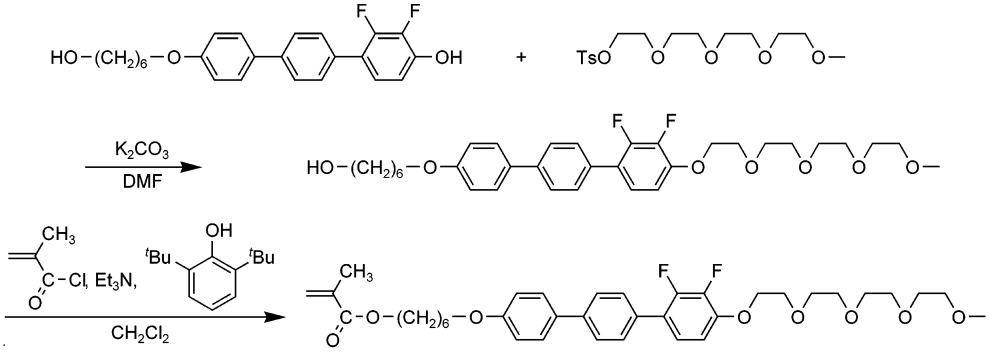

M1

Scheme 3. Synthesis of Liquid Crystalline Monomer **M2**

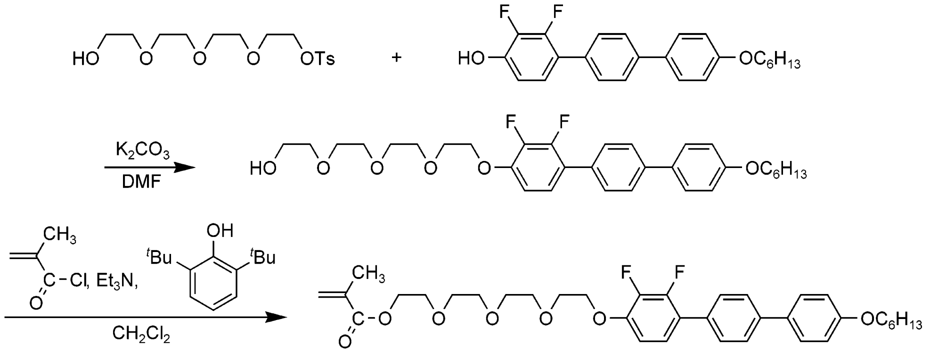

M2

Table 1. Phase Transition Temperatures of **M1** and **M2**, and the Lithium Salt Complexes of **M1**, **M2**, and **P1**−**P3**

compound	T_g[d]	$T_{solid-solid}$	$T_{solid-SmC}$	$T_{solid-SmA}$	$T_{SmC-SmA}$	$T_{SmA-Iso}$
M1[a]	−79		26		72	78
M2[a]	−71	50	72		80	105
M1/$LiOSO_2CF_3$[a,c]	−61	8	17		54	80
M2/$LiOSO_2CF_3$[a,c]	−65	49	67		75	112
P1/$LiOSO_2CF_3$[b,c]	−45			161		202
P2/$LiOSO_2CF_3$[b,c]	46		94		101	210
P3/$LiOSO_2CF_3$[b,c]	−44					

[a] Phase transition temperatures detected on the first cooling of DSC thermogram. [b] Phase transition temperatures detected on the second heating of DSC thermogram. [c] Lithium salt concentration: $[Li^+]/[CH_2CH_2O] = 0.05$. [d] Glass transition temperatures of the TEO moieties; abbreviations are as follows: SmC: smectic C phase, SmA: smectic A phase, Iso: isotropic phase.

were obtained by a palladium-catalyzed cross coupling reaction from 4-bromo-4′-alkoxybiphenyl derivatives and difluorophenylboronic acid compounds (Scheme 1). The methacryl group was introduced on the extremity of the alkyl chain for compound **M1**, while compound **M2** has the polymerizable group on the extremity of the TEO moiety.

Formation of Macroscopically Oriented Polymer Complexes. **M1** complexed with lithium triflate ($LiOSO_2CF_3$: 0.05 mol % to the ethylene oxide unit) showed smectic A (80−54 °C) and C phases (54−17 °C) on cooling, while **M1** alone exhibited a smectic A phase in a narrow temperature range (Table 1). The lithium salt complexes of **M1** aligned spontaneously on the glass or ITO substrates (Figure 3a, center). This monodomain of the oriented molecules was achieved by cooling from the isotropic to the smectic A phase. The uniform orientation was confirmed by the orthoscopic and conoscopic images taken with a polarized optical microscope (Figure 3a, center). This oriented liquid crystal in the smectic A phase at 60 °C was photopolymerized with UV irradiation (around 365 nm, 30 mW cm^{-2} for 20 min) in the presence of a photoinitiator, 2,2-dimethoxy-2-phenylacetophenone (0.5 wt %) (Figure 3a, right). A transparent film (**P1**/$LiOSO_2CF_3$) was obtained by this polymerization of the lithium salt complexes of **M1**. A cross-shaped pattern was also observed for the conoscopic image of the polymer complex, which indicates the preservation of macroscopic orientation after the polymerization (Figure 3a, right). The ^1H NMR spectrum for the polymer complex revealed that over 98% of the monomer were consumed through the reaction. For comparison, the oriented film of **P2** having the same aromatic core as **P1** was also obtained by the same method of alignment and polymerization for the lithium complex of **M2** (Figure 3b, and see Supporting Information). The film of **P3**/$LiOSO_2CF_3$ was prepared by casting the complex of lithium salt and the sample obtained by a solution polymerization in tetrahydrofuran (THF) using 2,2′-azobis(isobutyronitrile) as a radical initiator.

The phase behavior of the lithium salt complexes of **P1**−**3** is given in Table 1. The complex of **P1** and $LiOSO_2CF_3$ (0.05 mol % to the ethylene oxide unit) shows the LC smectic A phase up to 202 °C, which is 122 °C higher than that of the corresponding monomer complex. However, at room temperature, the polymer complex does not show any liquid crystalline phases and exhibits a solid phase below 161 °C. For the complex based on **P2**, the solid phase is observed below 94 °C.

The field emission scanning electron micrograph (FE-SEM) images of the cross-section for the film of **P1**/$LiOSO_2CF_3$ formed on the glass substrates show the formation of layered nanostructures (Figure 4). The average distance of the lines is

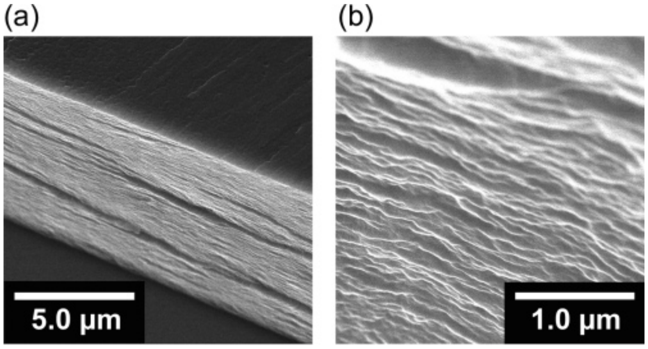

Figure 4. FE-SEM images of a macroscopically oriented **P1**/$LiOSO_2CF_3$ film. (a) Cross-section of the edge of the polymer complex film formed on the glass substrates. (b) Magnified view of the image in (a). The line textures aligned parallel to the substrates.

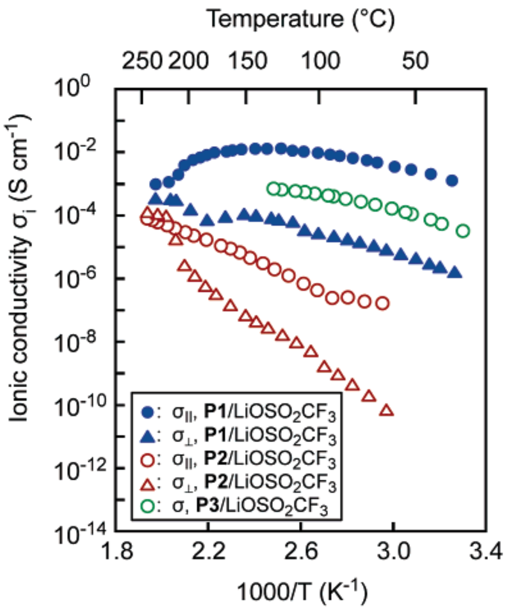

Figure 5. Anisotropic ionic conductivities of the polymer complexes of **P1**/ $LiOSO_2CF_3$ and **P2**/$LiOSO_2CF_3$ and ionic conductivities of the complex of **P3**.

estimated to be 10−50 nm. The layer spacing of the film measured using small-angle X-ray scattering of the polymer is 6.3 nm (see Supporting Information), suggesting that one line consists of several layers. These results show that the layered LC nanostructures of the monomeric complex were successfully locked in the solid-state polymer film by photopolymerization.

Anisotropic Measurements of Ionic Conductivity. The anisotropic ionic conductivities of the polymeric complexes were measured by the complex impedance method as previously reported.[18−21,25−29] Figure 5 presents ionic conductivities parallel ($\sigma_{\parallel}$) and perpendicular ($\sigma_{\perp}$) to the layer. The oriented complex of **P1** and $LiOSO_2CF_3$ shows high ionic conductivities in-plane direction of the smectic layers at room temperature. The $\sigma_{\parallel}$ value at 35 °C is 1.3×10^{-3} S cm^{-1}. At the same temperature, the $\sigma_{\perp}$ value is 1.8×10^{-6} S cm^{-1}, and the anisotropy in the ionic conductivities ($\sigma_{\parallel}/\sigma_{\perp}$) is about 7.5×10^{2}. The highest $\sigma_{\parallel}$ value of **P1**/$LiOSO_2CF_3$ is 1.4×10^{-2} S cm^{-1} observed at 150 °C in the oriented solid phase, while the $\sigma_{\perp}$ value is 1.1×10^{-4} S cm^{-1}. The $\sigma_{\parallel}$ values start to fall above this temperature, and the anisotropy in the ionic conductivities disappears in the isotropic phase. The $\sigma_{\parallel}$ values do not show sudden changes at the solid-smectic A phase transition. These results suggest that the ions can be transported faster in the well-oriented layer structures of the smectic A and ordered solid phases than in the isotropic liquids. It should be noted that the ionic conductivities of **P1**/$LiOSO_2CF_3$ are much higher than those of PEO-based LC or non-LC polymers (10^{-5}−10^{-4} S cm^{-1}).[16,17,22−37,39−42]

Chart 1

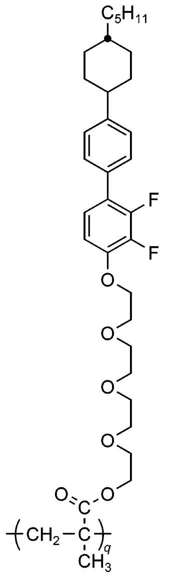

P4

To understand such high conductivities, the ionic conductivities of the lithium salt complexes of **P2** and **P3** were also measured (Figure 5).

The ionic conductivities perpendicular to the layer ($\sigma_{\perp}$) for the **P1**/$LiOSO_2CF_3$ complex are higher than those of the ionic conductivities parallel to the layer ($\sigma_{\parallel}$) for the **P2**/$LiOSO_2CF_3$ complex. The relatively higher values of $\sigma_{\perp}$ for the **P1** complex may be due to faster movement of ions within the layers.

The ionic conductivities parallel to the layer ($\sigma_{\parallel}$) of the **P2**/$LiOSO_2CF_3$ complex are lower than those of the complex of the analogous LC polymer **P4** having a cyclohexylbiphenyl mesogen previously reported (Chart 1).[25] For example, the $\sigma_{\parallel}$ value of **P2**/$LiOSO_2CF_3$ was 1.7×10^{-7} S cm^{-1} observed at 65 °C, which is one order lower than that of **P4**/$LiOSO_2CF_3$ observed at the same temperature (3.0×10^{-6} S cm^{-1}). The terphenyl mesogenic cores of **P2** may be packed more tightly with stronger intermolecular interactions than those of the cyclohexylbiphenyl cores of **P4**.

The highest ionic conductivities of the complex of **P1** at room temperature can be ascribed to the formation of nanoscale liquidlike layers in the solid film. The glass transition of the TEO moiety of the **P1**/$LiOSO_2CF_3$ complex is observed at −45 °C (Table 1). This observation shows that the TEO moiety is highly mobile even at around room temperature. The T_g of the complex of **P2** is seen at 46 °C, which is above room temperature. This shows that the segmental motion of the TEO chain of the **P2** complex is limited at room temperature.

---

(39) Kosonen, H.; Valkama, S.; Hartikainen, J.; Eerikäinen, H.; Torkkeli, M.; Jokela, K.; Serimaa, R.; Sundholm, F.; ten Brinke, G.; Ikkala, O. *Macromolecules* **2002**, *35*, 10149−10154.

(40) Imrie, C. T.; Ingram, M. D.; McHattie, G. S. *Adv. Mater.* **1999**, *11*, 832−834.

(41) Dias, F. B.; Batty, S. V.; Ungar, G.; Voss, J. P.; Wright, P. V. *J. Chem. Soc., Faraday Trans.* **1996**, *92*, 2599−2606.

(42) Brunsveld, L.; Vekemans, J. A. J. M.; Janssen, H. M.; Meijer, E. W. *Mol. Cryst. Liq. Cryst.* **1999**, *331*, 449−456.

The complex of non-LC polymer (**P3**) exhibits the same level of the glass transition temperature as the complex of **P1** (Table 1). However, the conductivities for **P3**/$LiOSO_2CF_3$ are lower than the $\sigma_{\|}$ values measured for the **P1** complex (Figure 5). This difference suggests that, in the self-organized conducting paths, ions can be transported more smoothly due to less entanglement and more cooperative motion of the grafted TEO chains from the mesogens (Figure 1c).

Conclusions

We have proposed a new strategy for high ion-conductive materials. The combination of the formation of nanolayers and grafting the chain from the aggregated mesogenic layers has been shown to be a promising approach for new highly ion-conductive organic soft materials. This nanostructured film exhibits not only high ionic conductivities but also two-dimensional ion conduction. The key to the formation of such oriented nanostructured film is to use the liquid crystalline alignment of the smectic phase followed by photopolymerization. The concept of nano-segregation of rigid and liquidlike layers may bring a new design of solid-state polymeric materials exhibiting transporting properties.

Experimental Section

Anisotropic Ionic Conductivity Measurements (complex impedance method). Dynamic ionic conductivities were measured using a Schlumberger Solartron 1260 impedance analyzer (frequency range: 10 Hz−10 MHz, applied voltage: 0.3 V) and a custom setup temperature controller (heating rate: 2.0 °C min^{-1}). Detection limits of resistance for the impedance analyzer were 10^2-10^8 Ω. The ionic conductivity was calculated to be the product of 1/resistance (Ω^{-1}) times cell constant (cm^{-1}). For anisotropic ionic conductivity measurements, two types of cells with comb-shaped gold (cell constant: 100 cm^{-1}) and ITO electrodes (cell constant: 0.1 cm^{-1}) were used (see Supporting Information). The ionic conductivities parallel ($\sigma_{\|}$) and perpendicular ($\sigma_{\perp}$) to the smectic layer direction were measured with gold and ITO cells, respectively.

Acknowledgment. This study was partially supported by Grant-in-Aid for Creative Scientific Research of “Invention of Conjugated Electronic Structures and Novel Functions” (No. 16GS0209) (T.K.) and Grant-in-Aid for Scientific Research (B) (No. 17350065) (T.K.) from the Japan Society for the Promotion of Science (JSPS) and Grant-in-Aid for The 21st Century COE Program for Frontiers in Fundamental Chemistry (T.K. and K.K.) from the Ministry of Education, Culture, Sports, Science, and Technology. K.K. is thankful for financial support from JSPS Research Fellowships for Young Scientists.

Supporting Information Available: Synthesis of liquid crystalline monomers and non-LC polymer **P3**, sample preparation of polymerizable complexes, photopolymerization, FE-SEM images of **P2**/$LiOSO_2CF_3$, X-ray charts, calculated molecular conformation, ionic conductivity measurement cells. This material is available free of charge via the Internet at http://pubs.acs.org.

JA0549594